

## EFFECTS OF SURFACE MORPHOLOGY ON THERMAL CONTACT RESISTANCE

by

**Haiming HUANG\* and Xiaoliang XU**

Institute of Engineering Mechanics, Beijing Jiaotong University, Beijing, China

Original scientific paper  
UDC: 66.018.4:536.24:517.96  
DOI: 10.2298/TSCI11S1033H

*The thermal contact resistance is common in aerospace industry, nuclear reactors and electronic equipments. The work addresses a new scheme for determining the thermal contact resistance between a smooth surface of a film and a rough surface of a metal specimen. The finite element method was used as a tool to explore the surface morphology effect on the thermal contact resistance while the temperature of the contact surface was determined by a regression method. According to the results developed, the temperature on the contact surfaces linearly drops with the increasing average height of surface roughness and nonlinearly drops with the increasing ratio between non-contact area and nominal contact area. On the other hand, the thermal contact resistance increases linearly with increases in the average height of the surface roughness. What's more, the thermal contact resistance increases in a non-linear manner as the ratio of the non-contact area to the nominal contact area is increasing.*

Key words: *thermal contact resistance, surface morphology, regression temperature, fractal*

### Introduction

When a heat flux conducts through two adjacent contact surfaces, an additional thermal contact resistance (TCR) appears at the contact region. The relationship of TCR with temperature, pressure, surface morphology and direction of heat flow is a complex and non-linear problem. TCR is a key factor in actual thermal design and relays to the uncertainty factors in thermal analysis. TCR analysis and determination is a hot topic in the contemporary literature addressing both simulation and experimental studies. In this context, Rao [1] reported a new method involving numerical heat transfer and parameter identification, while Amara *et al.* [2] used a random contact distribution and calculated TCR with a 3-D model. The approach of Shen *et al.* [3] utilizes different topological shapes to simulate the contact surfaces and yielded an approximate formula. Further, the Jackson's model [4] relates the effects of the scale dependent surface features and properties with the TCR. Chen *et al.* [5] measured TCR between grapheme and silicon dioxide by using a differential method. Wu *et al.* [6] found that the thermal resistances of porous materials could be effectively improved by adding appropriate number of interlayer of appropriate thickness.

\* Corresponding author; e-mail: hmhuang@bjtu.edu.cn

Although the surface morphology is known as a key factor of TCR [7], the roughness has been used only as a parameter in the previous studies [8] and little work has been done on the influence of surface morphology. Because of that, based on the fractal geometry [9-13] of the surface roughness, we report an investigation concerning the relationship between TCR and the contact surface morphology.

### Assumptions and scheme

TCR of the contacting surfaces is a combined result of the surface morphology, the thermo-physical properties of the contacting materials and the contacting loads. Among them, the surface morphology is of a primary importance. Generally, the actual contacts are series of discrete spots covering a wide range (10-60%) of the nominal contacting area, whilst the non-contact area encapsulates irregular pockets filled with gas or other medium. The heat flux passes only through the contact spots, as it is schematically illustrated by fig. 1, and depends on their areas.

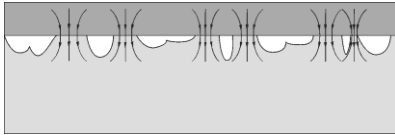


Figure 1. Physical mechanism of TCR

The simulations developed used three principle assumptions, among them:

- The physical properties of the contacting bodies within the areas of the spots are constant.
- The heat is transported only by conduction through the spots while any conduction or convection inside the pockets is ignored
- The bottom surface of the film facing the spots is completely smooth.

Based on the Rao's method [1] for measuring TCR between two specimens a scheme for determining TCR between a film and a specimen was developed in the reported study. Let us suppose that there is a metal specimen covered with a smooth film whose bottom temperature is  $T_m$ , and the bottom temperature of the specimen is kept as  $T_0$ , so the thermal conduction takes place through the contacting spots as it is shown schematically in fig. 2.

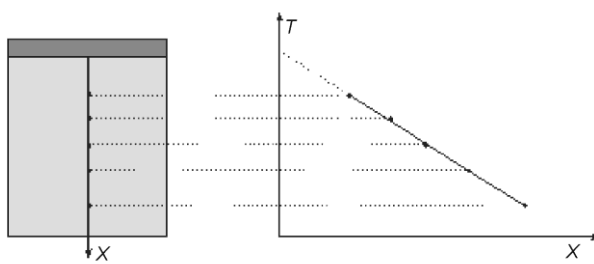


Figure 2. A scheme for calculating TCR between a film and a specimen

If the temperatures at equidistant points in the specimen are calculated, then the relationship  $T-X$  can be obtained with the linear regression method (see fig. 2). Further, then temperature  $T_r$  (defined by the regression relation-ship) at the top surface of specimen can be considered as one defined at  $X = 0$ . Hence, the temperature difference defining the flux through the contacting is:

$$\delta T = T_m - T_r \quad (1)$$

and TCR denoted as  $R_z$  can be read as:

$$R_z = \frac{\delta T}{q} = \frac{T_m - T_r}{q} \quad (2)$$

The heat flux  $q$  through the contact area can be determined either experimentally by a heat flow meter or calculated through numerical simulations using FEM. The present study refers to the second approach.

### Surface morphology

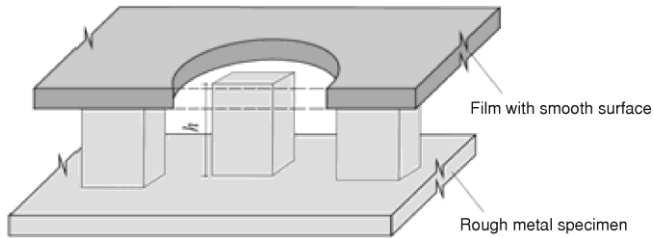


Figure 3. Factors of the surface morphology

Because the surface morphology is considered as the key factor of TCR we address mainly its effect to the TCR. Following the scheme in fig. 3, the surface morphology can be characterized by: the ratio between non-contact area and nominal contact area, and the average height of surface roughness, that is:

$$C_s = f(\lambda, h) \quad (3)$$

With eq. (3) the definition of TCR can be expressed as:

$$R_z = \frac{T_m - T_r(C_s(\lambda, h), P, T)}{q} \quad (4)$$

According to eq. (4), when the pressure  $P$  and the temperature  $T$  are given,  $R_z$  varies only with both  $\lambda$  and  $h$ .

### Simulation and results

Because the surface fractality is a natural the simulations considered an exploration of the morphology of the contacting surfaces through variation in only with  $\lambda$  and  $h$  creating various fractal surfaces. The Sierpinski gasket was used as a fractal object (see fig. 4).

With this simulated fractal object, let us suggest that, for instance, the temperature  $T_m$  of the film is about 1000 °C, while the bottom temperature  $T_0$  of the specimen is 0 °C and dimensions of the specimen:  $0.81 \times 0.81$  m. The thermal conductivity  $c$  and specific heat  $\zeta$  of specimen is 0.5 kWm/K and 2720 kJkg/K, respectively. Further, creating a surface morphology with  $h = 1$  mm and  $\lambda = 37.57\%$  and covering it by a smooth film, the heat flux distribution and the relevant TCR are calculated. The FEM were performed by dividing the object into 187,804 quad elements and consequent calculation of the temperature field by the software PATRAN and NASTRAN.

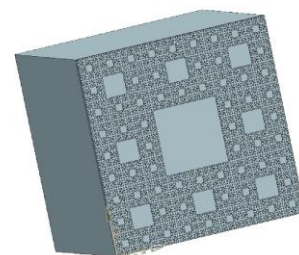


Figure 4. Roughness of contact surface based on the Sierpinski fractal

According to the results shown in fig. 5, the heat flux through the surfaces is not uniform due to incomplete contact area between film and specimen. The heat flux attains a

maximum in the area of largest depression and gradually reaches a uniform distribution on the bottom. The temperature field in fig. 6 indicates that the temperature over the depression area is lower than that at the contact surface. The larger depression corresponds to the larger temperature difference between depression area and contact surface.

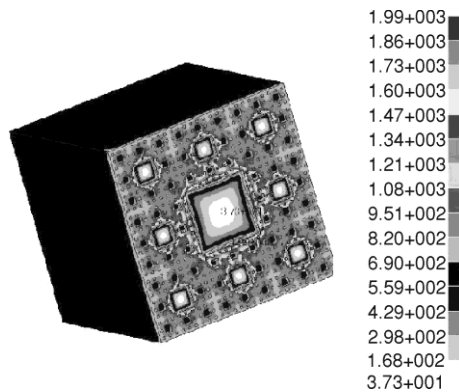


Figure 5. The heat flux distribution of specimen with  $h = 1$  mm and  $\lambda = 37.57\%$

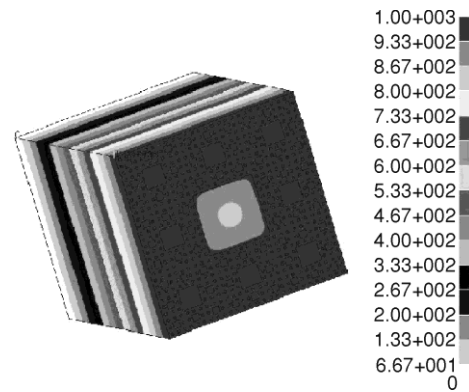


Figure 6. The temperature distribution of specimen with  $h = 1$  mm and  $\lambda = 37.57\%$

With variation in the value of the non-contact area ratio  $\lambda$  from 11.11% to 37.57% and  $h$  from 1mm to 4mm a series of simulations were performed. Some results of these numerical experiments concerning the regression temperature  $T_r$  and TCR defined by various  $\lambda$  and  $h$  are illustrated by figs.7(a, b).

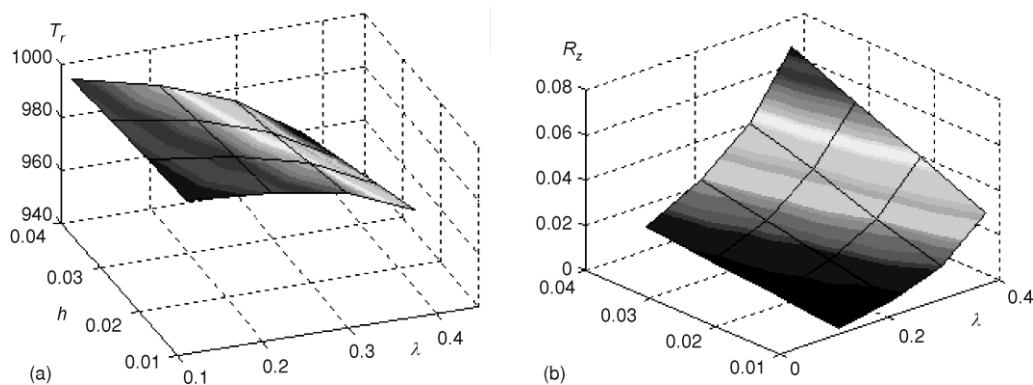


Figure 7. Effect of  $\lambda$ ,  $h$  on  $T_r$  or  $R_z$ , respectively; (a)  $T_r$ , (b)  $R_z$

The plots in figs. 8(a, b) demonstrate that, when  $\lambda$  is fixed, both TCR  $R_z$  and the regression temperature on the contact surfaces varies almost linearly with  $h$ , the regression temperature on the contact surfaces is inversely proportional to  $h$  and TCR  $R_z$  is proportional to  $h$ . Moreover, according to figs. 9(a, b), once the average height  $h$  is fixed, both TCR  $R_z$  and the regression temperature  $T_r$  on the contact surfaces vary nonlinearly as  $\lambda$  is increased, and the regression temperature on the contact surfaces decreases with the increasing  $\lambda$  while TCR  $R_z$  increases with the increasing  $\lambda$ .

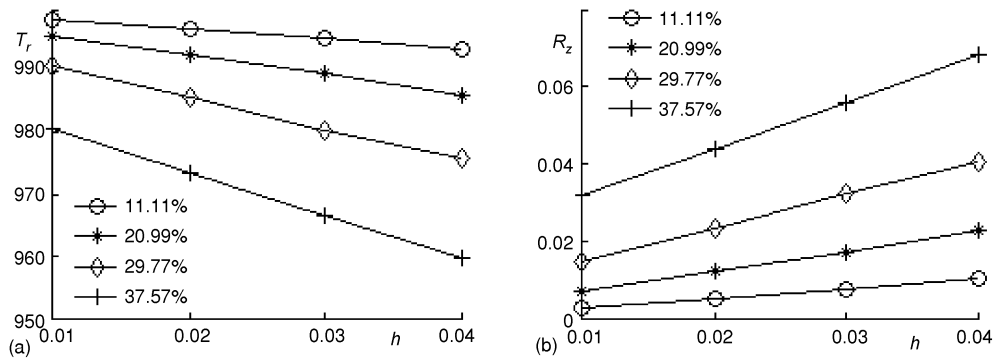


Figure 8.  $T_r$  and  $R_z$ , respectively, varies with  $h$ ; (a)  $T_r$ , (b)  $R_z$

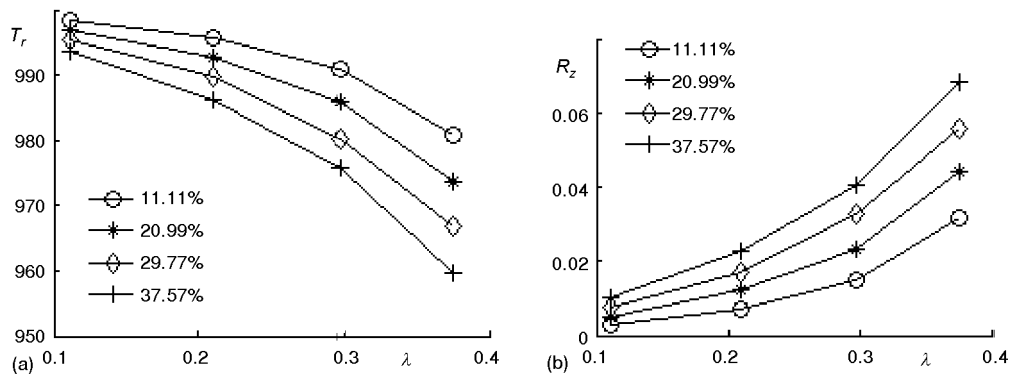


Figure 9.  $T_r$  and  $R_z$ , respectively, varies with  $\lambda$ ; (a)  $T_r$ , (b)  $R_z$

## Conclusions

This work addressed the relationship between surface morphology and TCR. Based on a fractal morphology simulated by the Sierpinski gasket, TCR of a metal specimen covered by a smooth film was calculated by FEM. The main results can be outlined as it follows:

- The regression temperature on the contact surfaces shows a linear decrease with the increasing average height of surface roughness.
- The regression temperature on the contact surfaces nonlinearly decreases with the increasing ratio between non-contact area and nominal contact area.
- TCR on the contact surfaces takes a linear increase with the increasing average height of surface roughness.
- TCR nonlinearly increases with the increasing ratio between non-contact area and nominal contact area.

## Nomenclature

$C_s$	– surface morphology, [–]	$q$	– surface heat flux, [ $\text{Wm}^{-2}$ ]
$h$	– average height of roughness, [mm]	$T$	– temperature, [K]
$R_z$	– thermal contact resistance, [ $\text{m}^2\text{KW}^{-1}$ ]		

*Greek letters*

$\lambda$	– ratio between non-contact area and nominal contact area, [–]	m	– bottom
		s	– surface
		z	– direction

*Subscripts*

r – regression

**References**

- [1] Rao, R. S., Identification Research on the Contact Thermal Resistance between Solid Samples Surface, *Industrial Heating*, 32 (2003), 2, pp. 16-18
- [2] Amara, M., et al., A 3D Computational Model of Heat Transfer Coupled to Phase Change in Multilayer Materials with Random Thermal Contact Resistance, *International Journal of Thermal Sciences*, 48 (2009), 2, pp. 421-427
- [3] Shen, J., Ma, J., Liu, W. Q., A Numerical Calculation Method of Thermal Contact Resistance, *Aerospace Shanghai*, 19 (2002), 4, pp. 33-36
- [4] Jackson, R. L., Bhavnani, S. H., A Multiscale Model of Thermal Contact Resistance between Rough Surfaces, *Journal of Heat Transfer*, 130 (2008), 8, pp. 081301.1-081301.8
- [5] Chen, Z., et al., Thermal Contact Resistance between Graphene and Silicon Dioxide, *Applied Physics Letters*, 95 (2009), 16, pp. 161910.1-161910.3
- [6] Wu, H. J., Fan, J. T., Du, N. Porous Materials with Thin Interlayers for Optimal Thermal Insulation, *International Journal of Nonlinear Sciences and Numerical Simulation*, 10 (2009), 3, pp. 291-300
- [7] Huang, H. M., Xu, X. L., Jiang, G. Q., Discrimination for Ablative Control Mechanism in Solid-Propellant Rocket Nozzle, *Science in China Series E*, 52 (2009), 10, pp. 2911-2917
- [8] Heichal, Y., Chandra, S., Predicting Thermal Contact Resistance between Molten Metal Droplets and a Solid Surface, *Journal of Heat Transfer*, 127 (2005), 11, pp. 1269-1275
- [9] Shi, X. J., Yu, W. D. Fractal Phenomenon in Micro-Flow through a Fiber Bundle, *International Journal of Nonlinear Sciences and Numerical Simulation*, 10 (2009), 7, pp. 861-866
- [10] Zhao, L., Wu, G. C., He, J.-H., Fractal Approach to Flow through Porous Material, *International Journal of Nonlinear Sciences and Numerical Simulation*, 10 (2009), 7, pp. 897-901
- [11] Yin, Y. J., et al., Centroid Evolution Theorem Induced from Fractal Super Fibers or Fractal Super Snowflakes, *International Journal of Nonlinear Sciences and Numerical Simulation*, 10 (2009), 6, pp. 805-809
- [12] Yin, Y. J., Yang, F., Fan, Q. S., et al., Cell Elements, Growth Modes and Topology Evolutions of Fractal Super Fibers, *International Journal of Nonlinear Sciences and Numerical Simulation*, 10 (2009), 1, pp. 1-12
- [13] Lai, P. J., Concise Methods to Generate Fractal Tilings, *International Journal of Nonlinear Sciences and Numerical Simulation*, 10 (2009) 5, pp. 585-595